Supplementary Information

Photodissociative Decay Pathways of the Flavin Mononucleotide Anion and its Complexes with Tryptophan and Glutamic Acid

Kelechi O. Uleanya, Cate S. Anstöter, and Caroline E. H Dessent*

Department of Chemistry, University of York, Heslington, York, YO10 5DD, UK.

ORCID ID

Kelechi O. Uleanya: 0000-0003-2017-1360

Cate S. Anstöter: 0000-0002-3412-2511

Caroline E. H. Dessent: 0000-0003-4944-0413

* Corresponding author:

Section S1: Laser Energy Measurements of $[FMN-H]^-$ Photodepletion

To explore the laser energy dependence of photodepletion of singly deprotonated flavin mononucleotide, $[FMN-H]^-$, precurosor ion depletion was measured as a function of photon energy (at 4.8, 4.4 and 3.5 eV). The results are shown in Figure S1a and reveal that photodepletion is linear over the range from 0-0.4 mJ. Photodepletion is saturated above ~1.0 mJ. To provide a comparison, we also present measurements for the singly and doubly deprotonated flavin adenine dinucleotide ions, $[FAD-H]^-$, and $[FAD-2H]^{2-}$, respectively, in Figures S1b and S1c. (The accompanying photodepletion spectra for the three ions are shown in Figure S2.) The laser energy dependencies are very similar for the three systems, illustrating that the flavin chromophore displays similar absorption properties in the three structurally similar molecules.

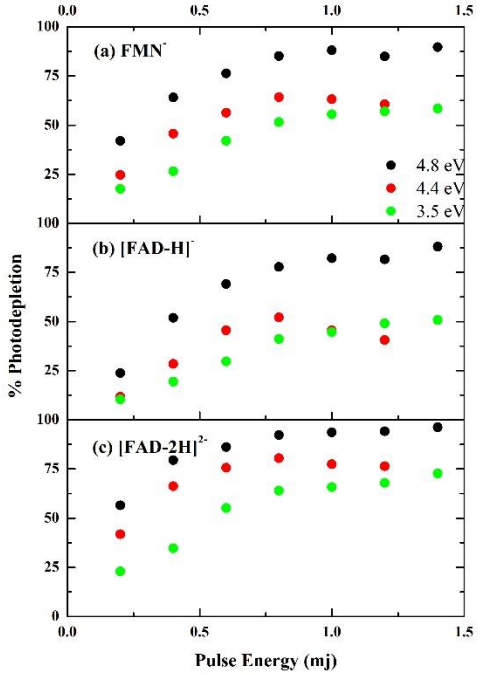

Figure S1: % Photodepletion of the $[FMN-H]^-$, $[FAD-H]^-$, and $[FAD-2H]^-$ molecular ions measured at 4.8, 4.4 and 3.5 eV as a function of laser pulse energy (mJ).

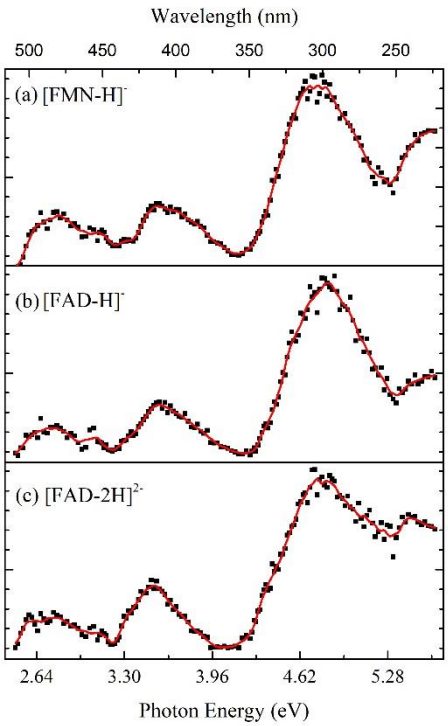

Figure S2: a) Photodepletion (gas-phase absorption) spectra of a) $[FMN\text{-}H]^-$, b) $[FAD\text{-}H]^-$, and c) $[FAD\text{-}2H]^-$, across the range 2.4 – 5.6 eV. The solid lines are five-point adjacent averages of the data points.

Section S2: Photofragment Action Spectra of $[FMN-H]^-$, $[FMN-H]^-$·TRP and $[FMN-H]^-$ ·GLU

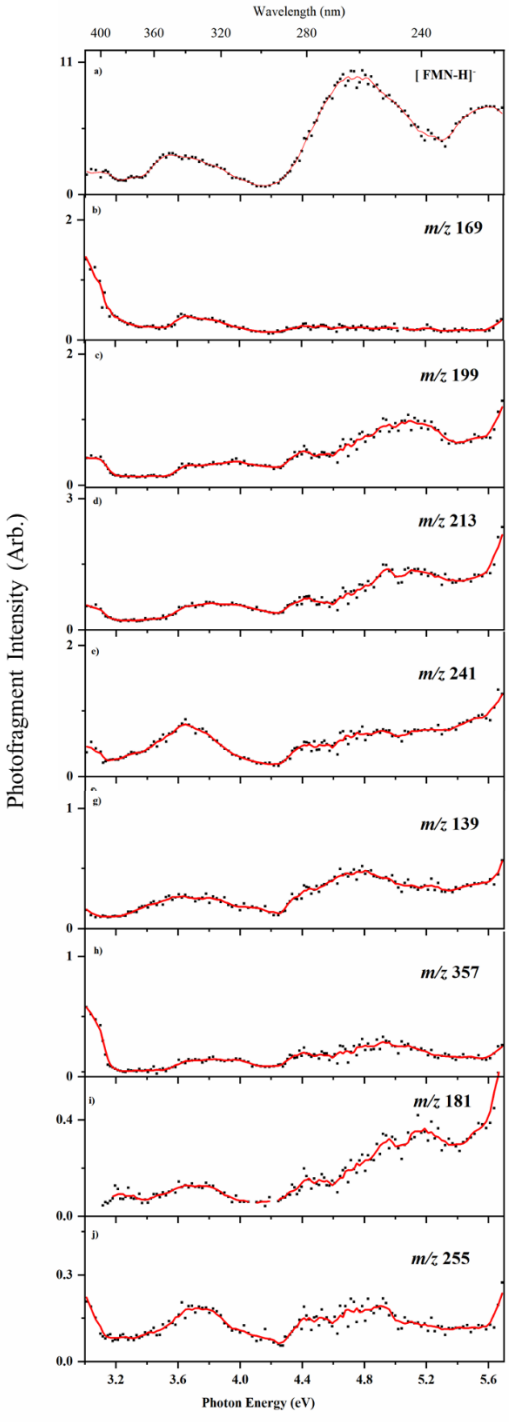

Figure S3: (a) Gas phase photodepletion spectrum of $[FMN- H]^-$, and (b-j) photofragment action spectra across the range 3.0 –5.7 eV. The solid line is a five-point adjacent average of data point.

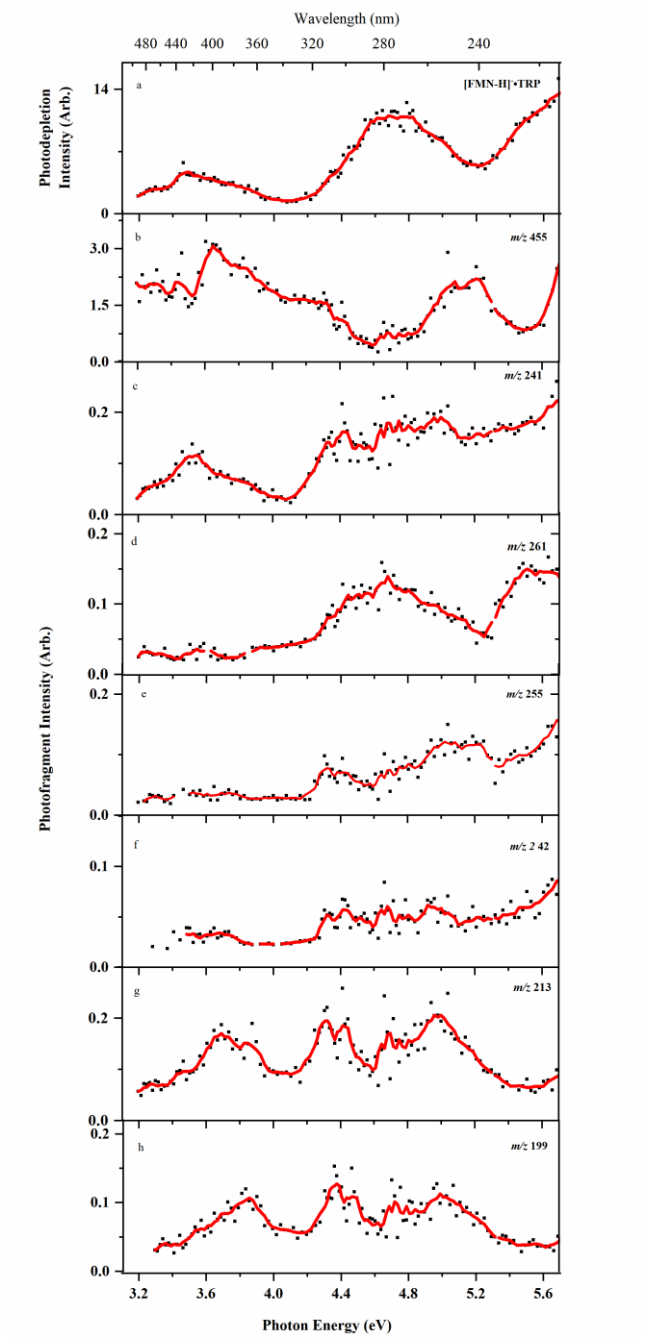

Figure S4: (a) Gas phase photodepletion spectrum of $[FMN\text{-}H]^{-}\cdot TRP$ and (b-h) photo fragment action spectra across the range 3.1-5.7 eV. The solid line is a five-point adjacent average of data point.

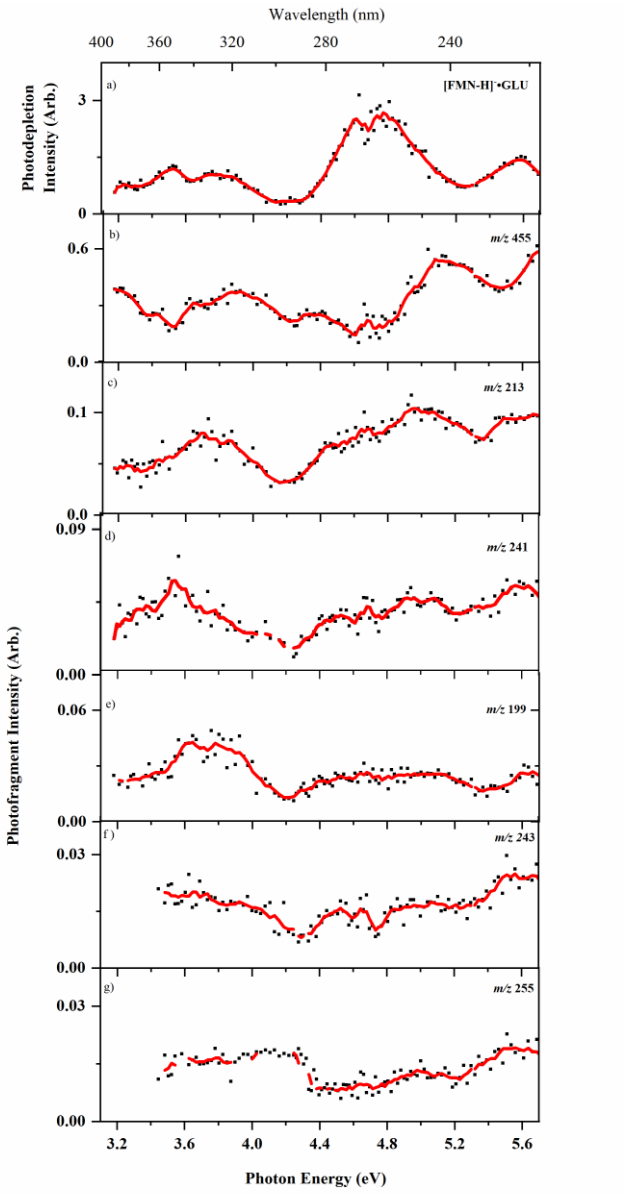

Figure S5: (a) Gas phase photodepletion spectrum of $[FMN\text{-}H]^{-}\cdot GLU$ and (b-g) photofragment action spectra across the range 3.1-5.7 eV. The solid line is a five-point adjacent average of data point.

Section S3: Electron detachment spectra of $[FMN-H]^-$, $[FMN-H]^-$·TRP and $[FMN-H]^-$ ·GLU complexes

While the laser-interfaced mass spectrometer employed in this work is not able to measure electron detachment yield directly, electron loss can be calculated assuming that any photodepleted ions that is not detected as an ionic-fragments are associated with electron loss. (Although our instrument only detect ions with m/z >50, these are generally a small proportion of the dissociative photofragment pathways for molecules of the size studied in this work.) In view of this, our calculated electron detachment yield represents the upper limit of the true electron detachment yield, therefore should be taken as an estimated value rather than an absolute value.

ED = (Photodepletion ion count -∑Photofragment ion count)/ (P*λ)

Where P = laser power

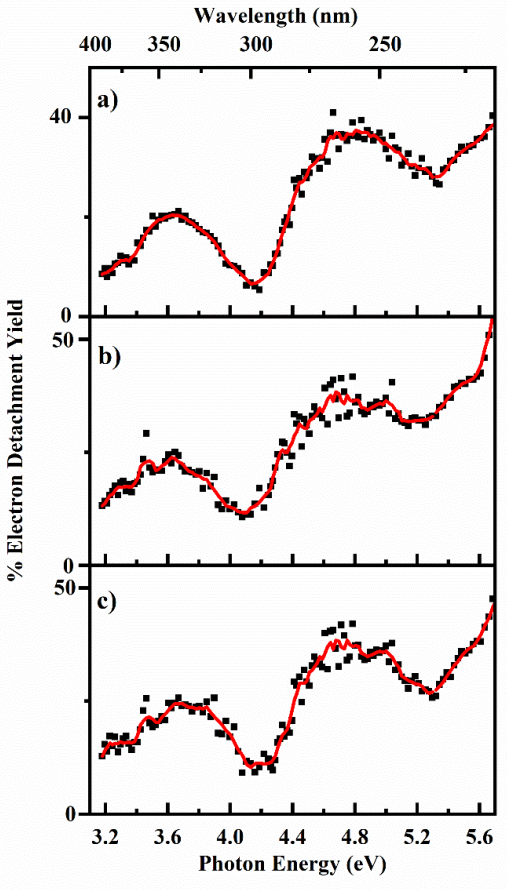

Figure S6: % Electron detachment yield spectra of a) $[FMN-H]^-$, b) $[FMN-H]^-$ ·TRP and c) $[FMN-H]^-$·GLU across the range 3.1-5.7 eV. The solid line is a five-point adjacent average of the data points.

Section S4: Geometric Structures of the [FMN-H]$^{-}$·TRP and [FMN-H]$^{-}$·GLU Complexes

[FMN-H]$^{-}$·TRP

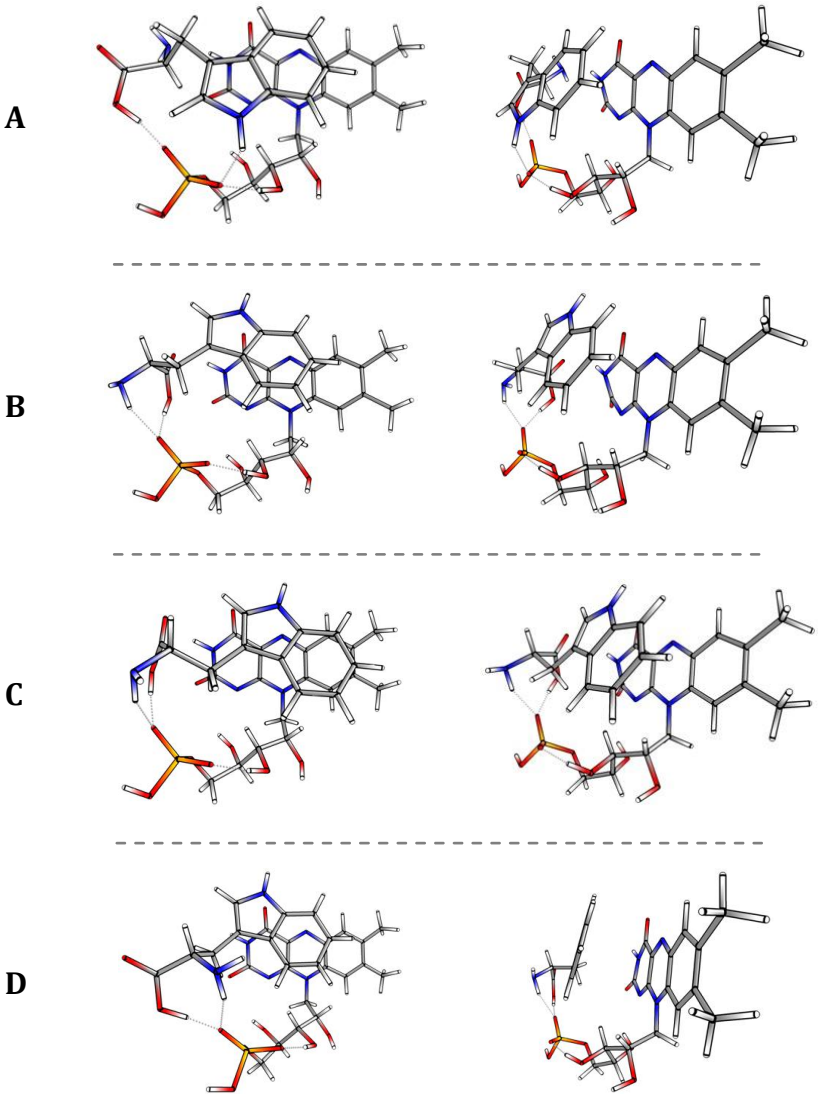

Figure S7: Geometric structures of [FMN-H]$^{-}$·TRP, displayed in order of increasing energy (**A-D**). See Table S1 for the associated energies.

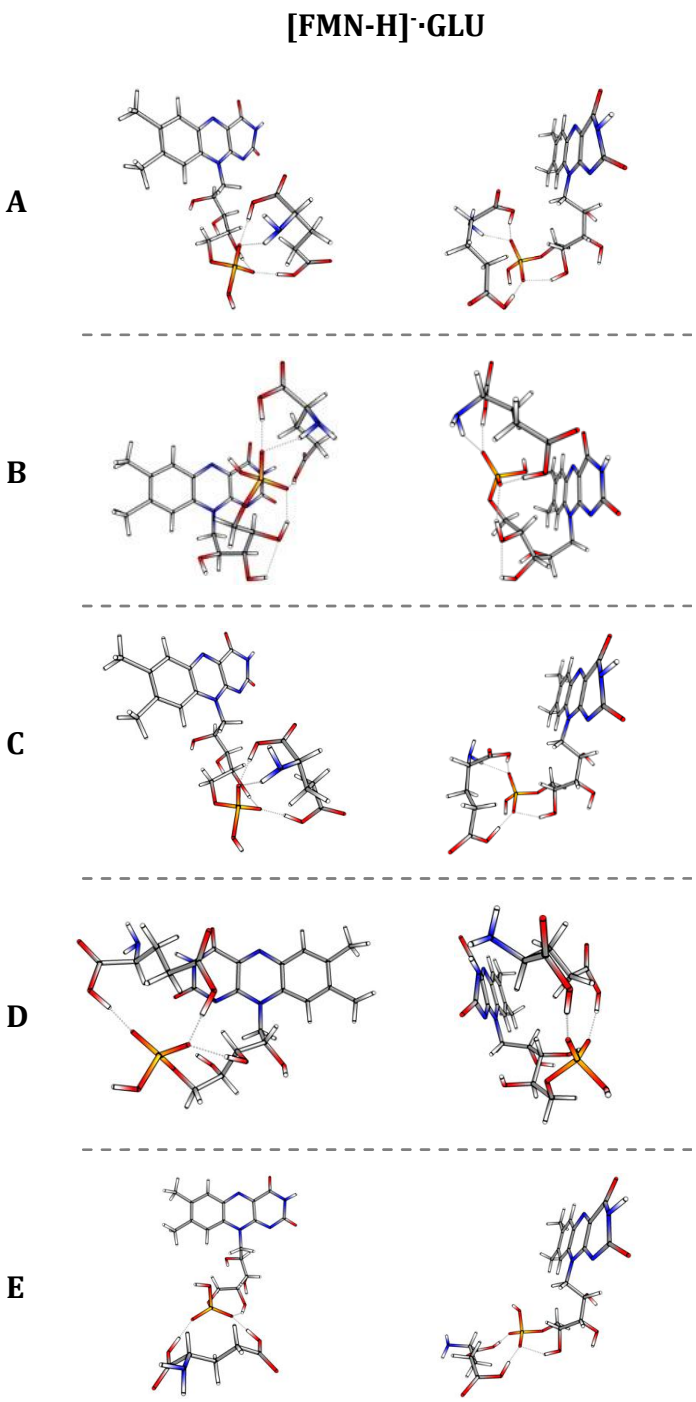

Figure S8: Geometric structures of [FMN-H]$^{-}$·GLU, displayed in order of increasing energy (**A**-**E**). See Table S1 for the associated energies.

Table S1: Calculated absolute and relative Energies (kJ/mol) for the $[FMN-H]^{-}$·TRP and $[FMN-H]^{-}$·GLU cluster structures illustrated in Figures S7 and S8. See main text for details of the calculations.

	Conformer	**Calculated Energy (kJ/mol)**	**Relative Energy (kJ/mol)**
$[FMN-H]^{-}$·TRP	**A**	-536.70	0.00
	B	-535.31	1.39
	C	-532.54	4.16
	D	-526.1	10.58
$[FMN-H]^{-}$·GLU	**A**	-815.3	0.00
	B	-806.6	8.75
	C	-805.8	9.49
	D	-805.5	9.78
	E	-803.35	11.97